Mon. Not. R. Astron. Soc. **000**, 1–10 (2002) Printed 29 January 2015 (MN LATEX style file v2.2)

Spectral analysis of BD+30°623, the peculiar binary central star of the planetary nebula NGC 1514⋆

A. Aller[1,2,3]†, B. Montesinos[1], L. F. Miranda[4,3], E. Solano[1,2], A. Ulla[3]
[1]*Departamento de Astrofísica, Centro de Astrobiología (INTA-CSIC), PO Box 78, E-28691 Villanueva de la Cañada (Madrid), Spain*
[2] *Spanish Virtual Observatory, PO Box 78, E-28691 Villanueva de la Cañada (Madrid), Spain*
[3]*Departamento de Física Aplicada, Universidade de Vigo, Campus Lagoas-Marcosende s/n, E-36310 Vigo, Spain*
[4]*Instituto de Astrofísica de Andalucía - CSIC, C/ Glorieta de la Astronomía s/n, E-18008 Granada, Spain*

Accepted 1988 December 15. Received 1988 December 14; in original form 1988 October 11

ABSTRACT
NGC 1514 is a complex planetary nebula with a peculiar binary central star (BD+30°623) consisting of a cool star and a hot companion. To date, the parameters of the two stars have not been firmly stablished. We present a detailed spectral analysis of BD+30°623 based on intermediate-resolution CAFOS optical spectra and IUE ultraviolet spectra with the goal of deriving the parameters of the two stars. For this purpose, we used an extensive composite grid of Kurucz and Tübingen NLTE Model-Atmosphere spectra. From the fitting procedure, in terms of the minimum χ^2 method, the best models obtained correspond to an Horizontal-Branch A0 star with $T_{\rm eff}$ = 9850±150 K, $\log g$ = 3.50±0.25, and a hot companion with $T_{\rm eff}$ between 80000 K and 95000 K and a $\log g \simeq 5.5$. To our knowledge, this is the first time that the parameters of both stars have been determined accurately through a detailed spectroscopic analysis.

Key words: planetary nebulae: individual: NGC 1514 – hot subdwarfs – stars: binaries – stars: fundamental parameters – techniques: spectroscopic

1 INTRODUCTION

Central stars of planetary nebulae (CSPNe) are evolved remnants of low- and intermediate-mass stars ($0.8 \leqslant M/M_\odot \leqslant 8$) and immediate precursors of white dwarf stars. Although they are key in the formation and evolution of their associated PNe, many aspects of CSPNe remain unknown by now. Among these, the binarity and its relationship with the properties of the nebulae is one of the most puzzling issues. According to Frew & Parker (2010) there are more than 3000 known galactic PNe. However, there is only spectroscopic information for ∼13% of their CSs (Weidmann & Gamen, 2011). Recent works show that just ∼ 40 of the exciting stars studied have been catalogued as binary CSs (de Marco et al. 2013). Therefore, there is still very little information concerning binarity in CSPNe which prevent us from constraining the formation and properties of these systems. In this context, many studies are being carried out with the aim of clarifying the role of binary stars in the formation of PNe (see, e.g., Miszalski et al. 2009).

There are many types of binary CSs but ones of special interest are those named *peculiar central stars* (Lutz 1977). This class refers to cool (spectral type A through K) CSs that are not hot enough to ionize their associated nebulae. Lutz suggested that these stars may belong to binary systems, where a hot (and faint) component would be the responsible for the photoionization while the cooler (and brighter) star would account for the absorption spectrum. Many works can be found regarding these stars (see, e.g, Méndez 1978, de Marco 2009, Pereira et al. 2010). However, the complexity of these systems makes their analyses difficult because the determination of the stellar parameters is laborious.

BD+30°623 (α = 04$^{\rm h}$ 09$^{\rm m}$ 16.$^{\rm s}$9, δ = +30° 46′ 33″, equinox 2000.0; ℓ = 165.°53, b = -15.°2), the exciting CS of NGC 1514, is one of these peculiar binary stars. It has been studied extensively but the physical parameters of the two components have not been determined accurately to date. It was initially classified as a single star and several spectral types were proposed in the literature ranging from B8 (Seares & Hubble 1920), to B9 (McLaughlin 1942) or A0 (Chopinet 1963). In contrast, Payne (1930) proposed an O8 classification.

Because of its peculiar spectrum, Kohoutek (1967) proposed, for the first time, the double star hypothesis for BD+30°623 based on photoelectric photometry. He reported the existence of a fainter and hotter companion and described the pair as A0 III + blue subdwarf (sdO) with effective temperatures ($T_{\rm eff}$) of 10800 K for the A-star and 60000 K for the hot star, and radii of 4.1$R_\odot$ and 0.45 $R_\odot$, respectively. Later, Kohoutek & Hekela (1967) confirmed these values based on a spectral analysis of the CS within the interval $\lambda\lambda$ 3650-5000 Å. In contrast, Greenstein (1972) reported that the ultra-

⋆ Based on observations obtained at the German-Spanish Astronomical Center, Calar Alto, jointly operated by the Max-Planck-Institut für Astronomie (Heidelberg) and the Instituto de Astrofísica de Andalucía (CSIC)
† E-mail: alba.aller@cab.inta-csic.es

violet luminosity of the sdO required a higher $T_{\rm eff}$ (100000 K), and that the cool star was, in fact, an Horizontal-Branch A star (A3-A5) with $T_{\rm eff} \leqslant 10000$ K. Further evidence of the binary nature of this system was provided by the International Ultraviolet Explorer (IUE) observations obtained by Seaton (1980). With these UV spectra and broad-band photometry from the Dutch ANS satellite, he constructed a model and described the system as an A0-A3 III star with $T_{\rm eff} \sim 9000$ K, and $\log g$= 3.0, and a hot star with $T_{\rm eff} \geqslant 60000$ K. To do this, he used a line blanketed model for the cool star and a blackbody for the hot companion. Besides, weak P Cygni profiles were detected. Later, Feibelman (1997) also used IUE spectra to report a considerable variability of the UV flux (by a factor of two) but he was not able to explain it. In strong contrast with previous determinations, Grewing & Neri (1990) used different methods to estimate $T_{\rm eff}$ of 27000, 28000, and 38000 K for the hot component. These values are too low to account for the observed He II emission from the nebula (Kaler 1976), which requires $T_{\rm eff}>$ 60000 K (see Pottasch 1984). In a most recent work, Taranova & Shenavrin (2007) proposed a spectral type B(3-7) main-sequence for the cool star based on infrared photometry. In these circumstances, it is clear that a new and detailed spectral analysis is necessary in order to determine the properties of this pair.

In this framework, we present an innovative spectral analysis of BD+30°623 by means of IUE ultraviolet and intermediate-resolution optical spectra. For this purpose, grids of synthetic spectra for the cool and hot stars were used and combined making use of the latest and state-of-the-art synthetic model-atmospheres. As far as we know, this is the first time that such analysis is done for one of these peculiar binary CSs.

2 OBSERVATIONS AND RESULTS

2.1 Intermediate-resolution optical spectra

Intermediate-resolution, long-slit spectra were obtained on 2011 January 16 with the Calar Alto Faint Object Spectrograph (CAFOS) at the 2.2-m telescope at Calar Alto Observatory (Almería, Spain). A SITe 2k×2k–CCD was used as detector. Gratings B-100 and R-100 were used to cover the 3200–6200 Å and 5800–9600 Å spectral ranges, respectively, both at a dispersion of $\simeq 2$ Å pixel^{-1}. The slit width was 2 arcsec and the spectra were obtained at two slit positions, both oriented north – south: one (denoted S1) with the slit centered on the CS and with an exposure time of 100 s for each grism; and another (S2) displaced ∼ 30 arcsec eastern from BD+30°623 and with an exposure time of 1800 s for each grism in order to cover the nebula. The projections of the slits on the sky are plotted in Fig. 1, which shows an [O III] (λ_0 = 5007 Å, FWHM = 87 Å) image of NGC 1514 also obtained with CAFOS in imaging mode. Seeing was $\simeq$ 2 arcsec during the observations.

The spectra were reduced with standard routines for long-slit spectroscopy within the IRAF and MIDAS packages. For the absolute flux calibration, the spectrophotometric standards G191B2B and Feige 34 were observed the same night. We note that the red part of the spectrum (above ∼ 6200 Å) presents an unexpected behavior that we were unable to correct in the flux calibration process. Therefore, the wavelength range beyond 6200 Å has not been taken into account for the analysis. However, the normalized uncalibrated spectrum at these wavelengths, in particular around Hα, is still usable to estimate the gravity of the cool component (see Sect. 4.2). Finally, we note that no problems with light losses in the flux calibration are present, since the available photometry in the blue part of the spectrum is compatible with our flux calibration.

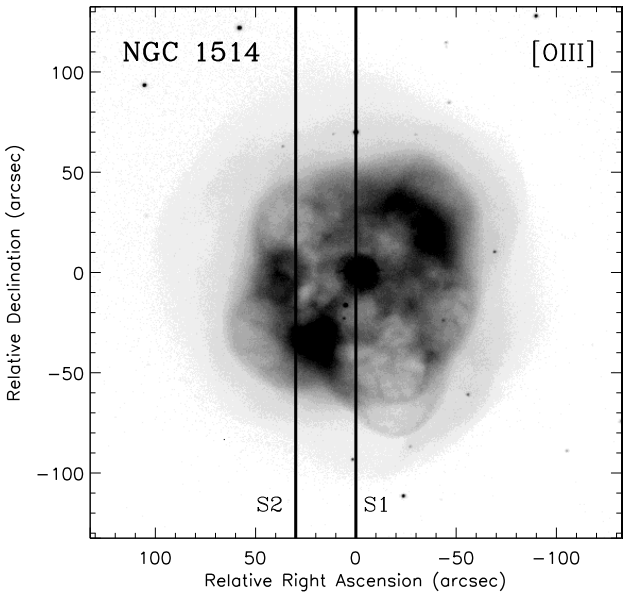

Figure 1. grey-scale reproduction of the [O III] image of NGC 1514. grey levels are linear. The two vertical lines S1 and S2 mark the slit positions used for intermediate-resolution, long-slit spectroscopy (see text).

The optical spectrum of BD+30°623 (Fig. 2), obtained at S1, shows strong hydrogen absorption lines which are typical of A- or B-type stars. The Ca II K λ3933 absorption line, also characteristic of these stars, is present. The spectrum also reveals other spectral features like He II λ4686 and λ5412 which are not expected in a typical spectrum of an A- or B-type star. They only appear (specially He II λ4686) in stars with $T_{\rm eff} \gtrsim 40000$ K (Eisenstein et al. 2006).

On the other hand, the spectrum shows very weak features of neutral helium. It is the case of He I λ4026 (whose contribution cannot be separated from that of He II λ4025 at this resolution) and He I λ4471 (that seems to be also present although with a smaller contribution). These neutral helium absorption lines may originate either from the cool star or from the hot companion. Once the spectral analysis is concluded (see Sect. 4) we will see that these neutral helium features come from the cool companion.

We note that no nebular emission lines are observed in Fig. 2 because of the very short exposure time of this spectrum (100 s), but they are clearly observed in the long-exposure spectrum obtained at S2 (Fig. 1). We used this spectrum (not shown here) to determine the logarithmic extinction coefficient c(Hβ). Because the Hα emission line flux is unreliable (see above), we used the integrated Hβ and Hγ fluxes observed at slit position S2 (see Fig. 1) to derive c(Hβ) $\simeq$ 0.97, assuming Case B recombination ($T_{\rm e}$=10^4 K, $N_{\rm e}$=10^4 cm^{-3}) and a theoretical Hγ/Hβ ratio of 0.466 (Osterbrock 1989). If we derive the colour excess from the relationship proposed by Seaton (1979) c(Hβ) = 1.47 $E(B-V)$, we obtain that E(*B*–*V*)= 0.66, in agreement with the value derived from the analysis of the CS (see Sect. 4.7). We also note that a slightly lower value for the logarithmic extinction coefficient (c(Hβ) = 0.885) was derived by Muthu (2001) from the observed Hα/Hβ ratio. Finally, the detection of the He II λ4686 emission line allows us to set a lower limit of $T_{\rm eff}$ = 60000 K for the hot companion (see above).

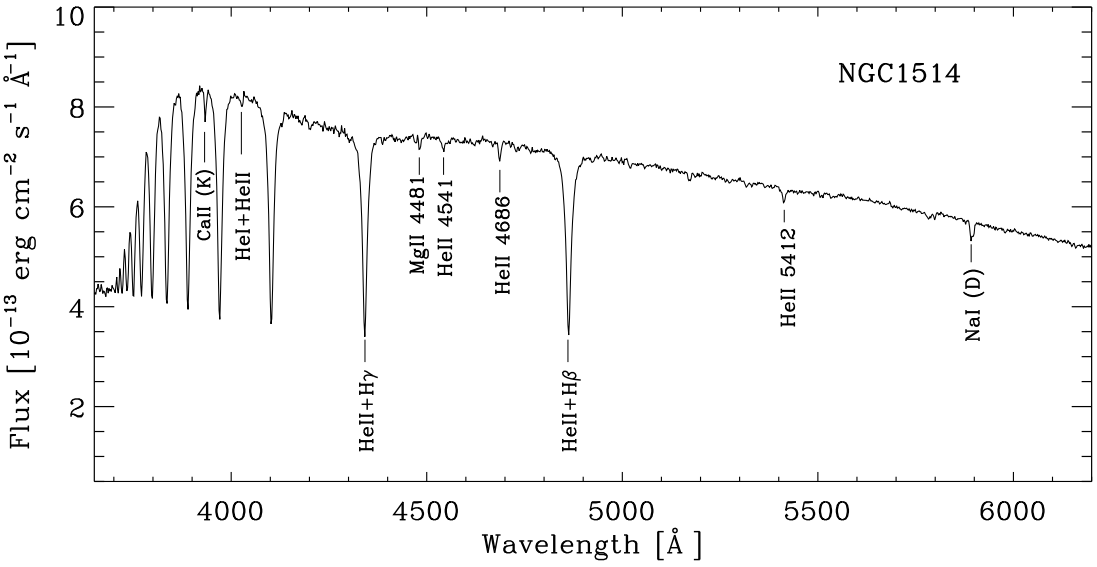

Figure 2. CAFOS CAHA blue spectrum of BD+30°623 in the range 3500–6200 Å. Some helium and hydrogen absorption lines are indicated, as well as the Ca II λ3968, and Mg II λ4481. The Na I doublet (λ5889-5895) is caused by interstellar absorption.

2.2 Low-resolution ultraviolet spectra

Since the $T_{\rm eff}$ of the hot companion of BD+30°623 should be higher than 60000 K, observations in the ultraviolet range are crucial to achieve a good characterization of this star. For this purpose, we have retrieved spectra from the International Ultraviolet Explorer (IUE) (Kondo et al. 1989) available in the IUE Newly Extracted Spectra (INES[1]) System. INES provides spectra already calibrated in physical units.

We have retrieved the available low-dispersion (~ 6 Å) IUE SWP (short wavelength) and LWP (long wavelength) spectra, which were obtained from 1978 to 1989. The SWP and LWP cover the ranges 1150-1975 Å and 1910-3300 Å, respectively. Only the pairs of spectra which were obtained consecutively, i.e., the same day were used. They are listed in Table 1. A mean of all spectra was calculated for the spectral analysis. Unfortunately, the LWP spectra beyond ~ 2400 Å could not be used since most of them appear to be saturated and/or with many bad pixels at those wavelengths.

Fig. 3 shows the SWP spectra listed in Table 1. Surprisingly, we have not found variability in the SWP spectra, in contrast with Feibelman (1997), who reported a variation in the flux of a factor ~ 2. In order to discard possible reduction errors in the INES spectra, the same IUE SWP spectra available from the MAST[2] archive were retrieved. These spectra are reduced in an independent way to that of the INES archive. No sign of flux variability was found in MAST spectra either. Therefore, we consider that the variability found by Feibelman (1997) should be reassessed.

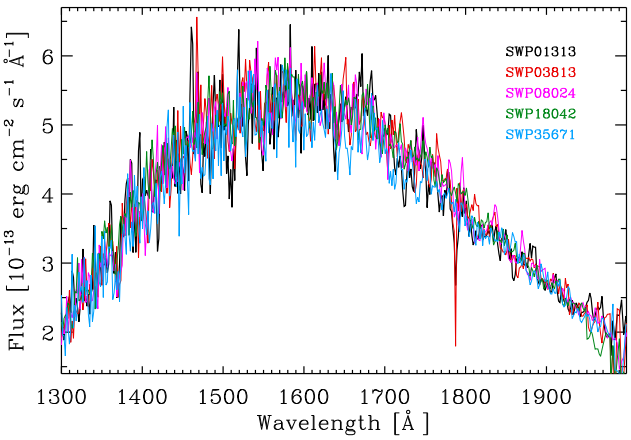

Figure 3. Plot of the five SWP spectra of BD+30°623 listed in Table 1 and used for the spectral analysis. No variability is observed in the SWP spectra, in contrast with that reported by Feibelman (1997).

3 SYNTHETIC STELLAR SPECTRA

In order to carry out an accurate spectral analysis of the composite spectrum of BD+30°623, three synthetic model atmosphere grids have been used.

For the cool component, high-resolution spectra were synthesized in the range 3000–8000 Å using the suite of programs SYNTHE (Kurucz 1993; Castelli & Kurucz 2003).

For the ultraviolet range (1150–3200 Å), low-resolution models from the ATLAS9 grid of model atmospheres[3] by Castelli & Kurucz (2003) were used. Finally, each ultraviolet spectrum was combined with the corresponding optical one to build a grid in the range of 1150-8000 Å.

[1] http://sdc.cab.inta-csic.es/ines/
[2] https://archive.stsci.edu/iue/search.php
[3] http://user.oat.ts.astro.it/castelli/grids.html

Table 1. IUE spectra used for the spectral analysis. The LWP spectra beyond ~ 2400 Å could not be used for the spectral analysis (see the text).

Spectrum	Date (dd/mm/yyyy)
SWP01313 + LWR01279	04/04/1978
SWP03813 + LWR03394	05/01/1979
SWP08024 + LWR06984	23/02/1980
SWP18042 + LWR14219	20/09/1982
SWP35671 + LWR15127	04/03/1989

For the hot component, we used TMAW[4], a service recently developed in the framework of the German Astrophysical Virtual Observatory (GAVO), to calculate theoretical stellar spectra of hot, compact stars. The service provides access to TMAP[5] (Tübingen NLTE - Model Atmosphere Package; Werner et al. 2003), a collection of models successfully used for spectral analysis of hot, compact stars (e.g, Rauch et al 2007, 2013; Ziegler et al. 2012).

We requested for a H+He, high-resolution grid, via TMAW, with 50000 K $\leqslant T_{\rm eff} \leqslant$ 120000 K in the range 1000 – 55000 Å. The spectral resolution was 0.1 Å in the range 1000 – 8000 Å and 1 Å in the rest of the wavelengths. Since the H and He lines are not very sensitive to $T_{\rm eff}$ beyond 70000 K, we sampled from 50000 K to 70000 K in steps of 2000 K and from 70000 K to 120000 K in steps of 5000 K. Surface gravity in this grid ranges from $3.0 \leqslant \log g \leqslant 7.0$ in steps of 0.2 dex. However we note that those models above the Eddington limit could not be calculated with the TMAW procedure. Therefore, the lower limit in $\log g$ is in fact set by the Eddington limit. The abundance ratio (by mass) of hydrogen to helium was varied as follows: H/He = 1/0, 0.9/0.1, 0.8/0.2, ..., 0.1/0.9, 0/1. No other elements have been taken into account for the calculation.

Before starting the spectral analysis, the synthetic spectra were degraded and rebinned to the resolution of the observations, which is $\simeq 2$ Å pixel^{-1}.

4 SPECTRAL ANALYSIS

4.1 Composite models

The observed flux of a composite spectrum can be reproduced by the sum of two terms, each one referring to each individual spectrum, following the relation:

$$F_\lambda = \left(\frac{R_{\rm cool}}{d}\right)^2 S_\lambda(T_{\rm eff(cool)}, g_{\rm cool}) + \left(\frac{R_{\rm hot}}{d}\right)^2 S_\lambda(T_{\rm eff(hot)}, g_{\rm hot})$$
$$= k_{\rm norm}[S_\lambda(T_{\rm eff(cool)}, g_{\rm cool}) + a\, S_\lambda(T_{\rm eff(hot)}, g_{\rm hot})] \quad (1)$$

where $R_{\rm cool}$, $T_{\rm eff(cool)}$, $g_{\rm cool}$, $R_{\rm hot}$, $T_{\rm eff(hot)}$, $g_{\rm hot}$ are the radius, the $T_{\rm eff}$ and the surface gravity of each object, d is the distance to the system (assuming that both objects are at the same distance) and S_λ the monochromatic surface flux emission of each component. In this way the parameter a is defined as $(R_{\rm hot}/R_{\rm cool})^2$ and $k_{\rm norm}$ is the normalization constant defined as $(R_{\rm cool}/d)^2$. Each composite model will be normalized to the observed spectrum following the procedure described by Bertone et al. (2004).

The last term of equation (1) has five unknowns, namely both $T_{\rm eff}$ and gravities, and the parameter a. In addition, the extinction affecting the observed spectrum –both R_V and $E(B-V)$– is also unknown. This amounts to a total of seven unknowns, which poses a difficult problem to be tackled. Therefore, to arrive the final and sensible solution(s) we have devised a method to explore the whole range of parameters by building a grid of composite models from the individual grids, and by applying a suite of filters that allows us to select, among all possible combinations, those matching the observed spectral features, both at an overall level (the shape of the spectrum, the position of the Balmer jump) and lines (equivalent width of some absorption lines). The outcome of the analysis will be the $T_{\rm eff}$, gravities and the ratio between the radii of the components.

In what follows we will explain in detail the fitting procedure, until the final solutions are reached. Fig. 4 shows a flowchart describing the whole process. Note that an iterative process is needed because each cycle hinges on the parameters of the cool component that must be revised once each iteration is completed, until convergence is reached.

4.2 Parameters of the cool component

As it can be seen in Fig. 4, and is described in detail in the next subsections, the whole fitting process is based on the computation of grids of composite models where, in each one, the Kurucz synthetic spectrum of the cool star remains fixed and it is combined with all the TMAP models. The composite models undergo several filters imposed by the observations and only the small subset that fulfills all the observational constraints is accepted as a final solution for the problem. Therefore, the first step is to constrain the parameters of the cool star. These parameters are reassessed at the end of each cycle. We note that an approach from the point of view of the hot star (i.e, fixing the parameters of the hot star and combining with the whole grid of the Kurucz models) is not possible since we do not have enough spectral criteria to adjust the corresponding pairs of $T_{\rm eff}$ and gravity for the hot component.

The Ca II K λ3933 line is generally one of the prime temperature criteria in A- or B-type stars (Gray & Corbally, 2009). In the case of single stars, an estimate of $T_{\rm eff}$ can be obtained by comparing the equivalent width (EW) of the line in the observed spectrum with that measured on a grid of synthetic spectra or templates. However, this simple procedure cannot be applied in this case, because superimposed to the spectrum of the cool component, there is an unknown contribution of the continuum and lines of the hot component. The only information we can extract in the first step is an upper limit to the $T_{\rm eff(cool)}$, since composite models –or combinations of templates– containing a cool star whose EW(Ca II) $\leqslant$ 0.34 Å (which is the EW of the line in the observed spectrum) will have the EW of this line decreased below that value when the spectrum of the hot companion is added. An inspection of the grid of synthetic models (see Sect. 3) with solar metallicity sets a rough upper limit of $T_{\rm eff(cool)} \sim$11000 K. The Ca II K line dependence on gravity and metallicity was found negligible.

Since the wings of the Balmer lines are very sensitive to gravity in A- and B-type stars (Gray & Corbally, 2009), we have explored which value of $\log g$ for the cool component is consistent with each potential $T_{\rm eff}$. We have computed synthetic models for Hα, Hβ, Hγ and Hδ for $T_{\rm eff(cool)}$=9000 – 11500 K, in steps of 500 K, and values of $\log g_{\rm cool}$=2.50 – 4.00, in steps of 0.25 dex. Such intervals were chosen according to the typical parameters of A- and B-type stars. The widths of the lines in the spectrum have been compared with those in the synthetic models, and the pairs ($T_{\rm eff(cool)}$, $\log g_{\rm cool}$) that are consistent with the observations are (9000 K,

[4] http://astro.uni-tuebingen.de/~TMAW/
[5] http://astro.uni-tuebingen.de/~TMAP/

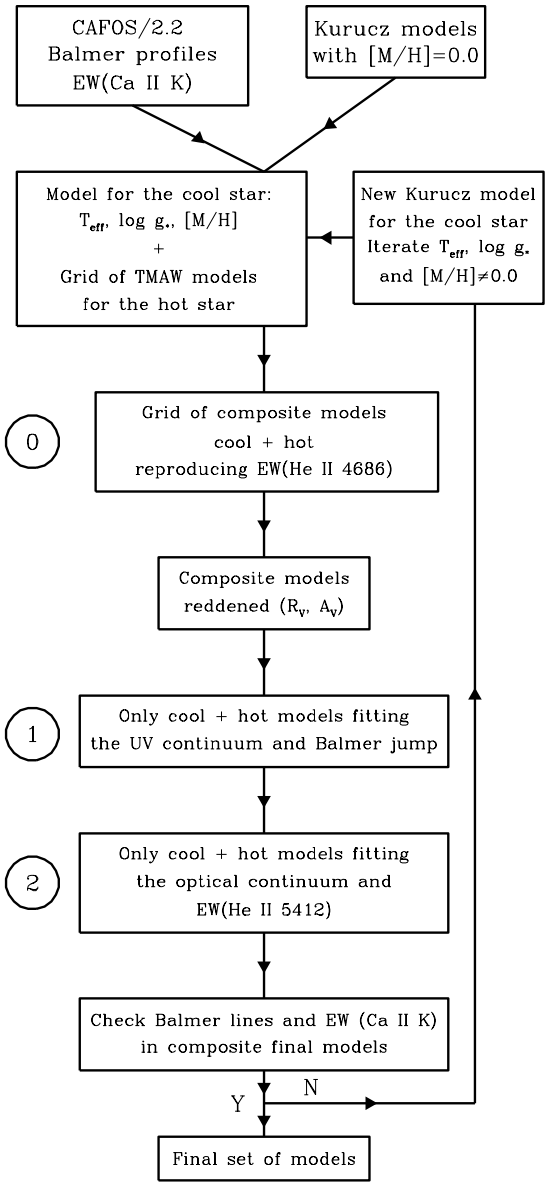

Figure 4. Flow chart with all the steps of the fitting procedure. See text for details.

2.50), (9500 K, 2.75), (10000 K, 3.00), (10500 K, 3.25), (11000 K, 3.50) and (11500 K, 3.75). Typical errors in the determination of $\log g_{\rm cool}$ are ±0.25 dex.

We would like to stress that we are comparing models computed with a single $T_{\rm eff}$ and gravity with the observed spectrum, that is a composite of two stars. The assumption underlying this exercise is that the cool component is the main contributor to the Ca II K and the Balmer lines. We also note that a possible interstellar contribution to this absorption line was not taken into account in the analysis. Although the low-resolution of our spectrum does not allow us to quantify this contribution, Greenstein (1972) concluded that the cool component has a considerable strong stellar line by comparing the velocity of the observed Ca II K line and the expected interstellar line velocity.

Once the complete filtering process is done and the contributions of both components to the observed spectrum are evaluated, the Ca II K line and the Balmer profiles are analyzed again and the values of $T_{\rm eff(cool)}$ and $\log g_{\rm cool}$ are reassessed to fit the observations (see Sect. 4.5). The whole fitting and filtering process is started again (see Fig. 4).

4.3 First filter: UV continuum and Balmer jump

Before starting with the filtering procedure, we imposed the condition that the EW of the He II λ4686 line of *all* composite models matches that of the observed line, namely $\sim$ 0.42 Å. Therefore, for each pair $S_\lambda(T_{\rm eff(cool)}, g_{\rm cool})$, $S_\lambda(T_{\rm eff(hot)}, g_{\rm hot})$, the parameter $a(T_{\rm eff(cool)}, T_{\rm eff(hot)}, g_{\rm cool}, g_{\rm hot})$ is computed in such a way that the synthetic EW matches the observed one. The outcome of this step, –marked as '0' in Fig. 4– is a grid of composite models that will be passed to the first filter.

Since the ultraviolet and blue wavelengths are the most sensitive to the interstellar and nebular extinction, we carried out first an initial analysis fitting only the UV shape and the Balmer jump. To do this, we explored a wide range of reddening values and applied those to the models. In principle we shall not assume the unique Galactic average value of 3.1 for R_V (see Sect. 5 for further discussions) then, we varied this parameter and the colour excess $E(B–V)$. The values adopted for this analysis range from 1.5 to 5.0 in steps of 0.1 in the case of R_V, and from 0.2 to 1.5 in steps of 0.05 in the case of $E(B-V)$. The parameterization of the extinction by Fitzpatrick (1999) has been used.

A least squares fit with a confidence level of 99.73% (3σ), yields a first effective filtering over the total grid. We obtained that only those models with $E(B-V)$ between 0.5 and 0.6 and R_V between 2.3 and 2.6 fitted well the UV shape, and pass to the next filter. This step is marked as '1' in Fig. 4.

4.4 Second filter: optical continuum and He II λ5412

After the first filter, we performed a second fitting –'2' in Fig. 4– to match the optical continuum. Once again, a least squares fit with a confidence level of 3σ was carried out. At this point, we also imposed the requirement of a good fitting to the He II λ5412 absorption line.

4.5 Reassessment of the parameters of the cool star

As mentioned in Sect. 4.2, in the first iteration we repeated the fitting procedure keeping fixed all the pairs ($T_{\rm eff(cool)}$, $\log g_{\rm cool}$) of the cool star that seemed to be compatible with the observations, combining them with the whole grid of synthetic spectra for the hot star.

After that first iteration, the EW of the Ca II K line and the widths of the wings of the Balmer lines were measured on each of the composite spectra that passed all the filters. As expected, the EW of the Ca II line is less, and the wings of the Balmer lines were narrower, than those in the observed spectrum –and on each of the individual models with ($T_{\rm eff(cool)}$, $\log g_{\rm cool}$)– due to the fact that a contribution of the hot component had been added to each cool model. The comparison of the features of the composite spectra with those observed helped to tune the parameters of the cool star. A new iteration was then started with the revised set of parameters, as shown in Fig. 4.

After a few cycles it turns out that convergence in the procedure, and an excellent agreement with the observed spectrum, are achieved for $T_{\rm eff(cool)} = 9850 \pm 150$ K and $\log g_{\rm cool} = 3.50 \pm 0.25$.

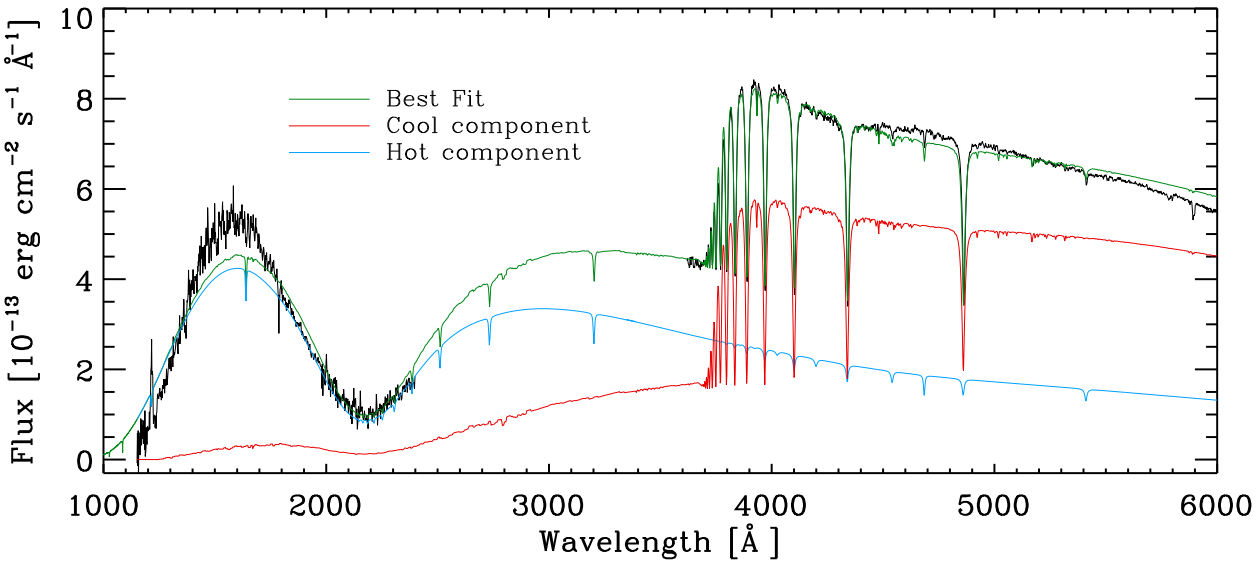

Figure 5. Observed spectrum of BD+30°623 (black) and one of the best fits (green) chosen between the models for the hot component that pass the filters described in Sect. 4, which corresponds to $T_{\rm eff(hot)}$ = 90000 K, log $g_{\rm hot}$ = 5.6 and H/He= 0.4/0.6. The parameters for the cool component are $T_{\rm eff(cool)}$ = 9850 K and log $g_{\rm cool}$ = 3.5. All the other solutions are virtually identical and are not plotted to avoid confusion. In red and blue the separate contributions of the cool and hot stars, respectively, are plotted.

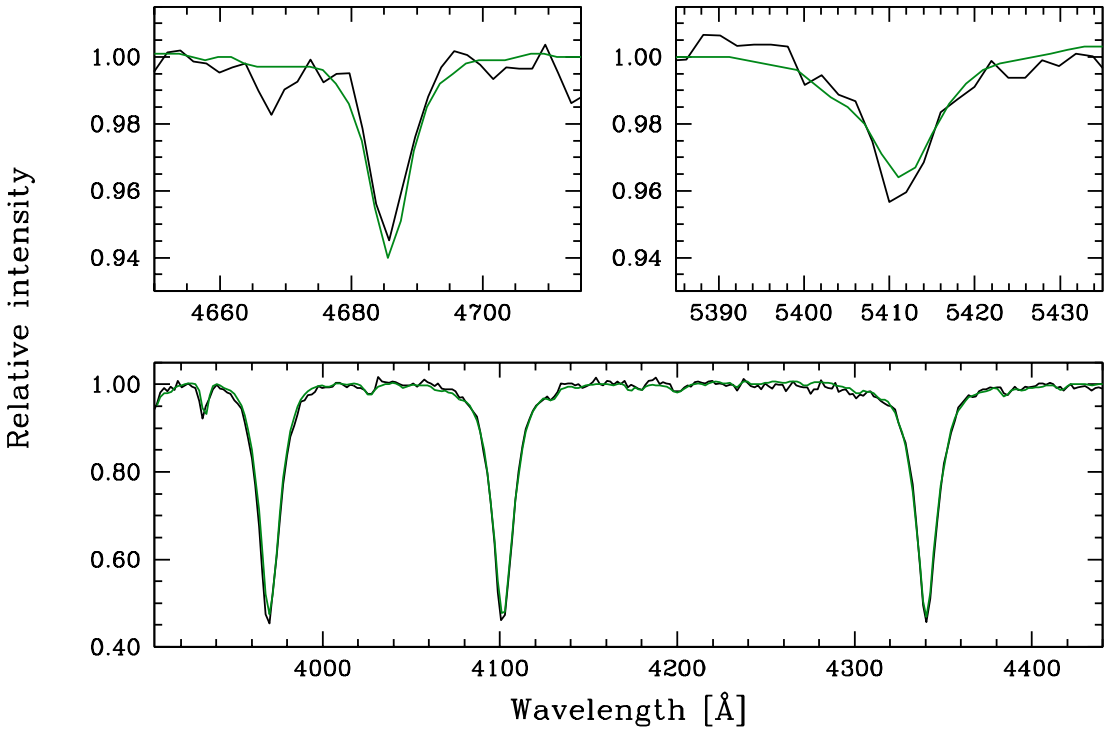

Figure 6. Profiles of the observed absorption lines (black) used for the spectral analysis together with the synthetic profiles (green) of one of the final solutions. In the upper part of the figure the He II λ4686 and He IIλ5412 lines. In the lower part, the Ca II K line and the Balmer lines Hϵ, Hδ and Hγ.

Table 2. Spectroscopic solutions for the hot component of BD+30°623.

$T_{\rm eff(hot)}$ [K]	$\log g_{\rm hot}$	H/He	a
80000	5.4	0.6/0.4	0.01445
85000	5.6	0.5/0.5	0.01328
90000	5.6	0.4/0.6	0.01211
95000	5.6	0.0/1.0	0.01172
95000	5.6	0.2/0.8	0.01113
95000	5.6	0.3/0.7	0.01113
95000	5.6	0.4/0.6	0.01094

These parameters are compatible with both an A0 star ascending the giant branch (as reported by, e.g, Kohoutek 1967) and a Horizontal-Branch (HB) A0 star (as reported by Greenstein 1972). We will see below that the HB A0 classification appears to be the most probable one. The strength of the Ca II K and other weak blends point to a subsolar metallicity. A value of $[{\rm M/H}]_{\rm cool} = -0.5$, which seems to match the observed features, has been adopted; however, high-resolution spectra would be needed to confirm or reject this.

4.6 Final results for the hot star

For that particular set of parameters of the cool star, seven successful solutions were obtained for the hot companion, with $T_{\rm eff(hot)}$ between 80000 K and 95000 K, $\log g_{\rm hot}$ between 5.4 and 5.6 and compositions compatible with a helium-rich star (H/He= 0.0/1.0, 0.2/0.8, 0.3/0.7, 0.4/0.6, 0.5/0.5, 0.6/0.4). These final solutions together with the corresponding values of the parameter a (see Eq. 1) are listed in Table 2. The derived stellar parameters are compatible with most of the different known types of CSPNe, so we would need more information (e.g., mass, radius, luminosity) to classify the hot component in a definitely way (see Sect. 5).

Fig. 5 shows one of these final solutions, namely that with $T_{\rm eff(hot)} = 90000$, $\log g_{\rm hot} = 5.6$ and H/He= 0.4/0.6, plotted in green. All the other solutions are virtually identical and are not included in the figure to avoid confusion. We have also plotted the individual contributions of the cool and hot stars in red and blue, respectively. As mentioned in Sect. 2, the neutral helium lines (e.g., He I λ4471) come from the cool companion. This is in agreement with the high $T_{\rm eff}$ derived for the hot star.

In Fig. 6 the profiles of the He II λ4686, He IIλ5412, Balmer lines Hϵ, Hδ and Hγ, and Ca II K line, together with the corresponding fits are shown.

4.7 Extinction

As it can be seen in Fig. 4 and Sect. 4.3, each composite model is reddened with a range of values of R_V and colour excess $E(B-V)$ to match the shape of the UV continuum and the intensity of the Balmer jump. All final models matching successfully the observed spectrum had to be reddened with values of $R_V = 2.3 \pm 0.1$ and $E(B-V) = 0.60 \pm 0.05$, which imply $A_V \simeq 1.4$. Note that the value of the extinction does not have any impact on those filters matching the EW of lines, since on narrow regions around absorption lines the extinction correction can be considered as constant and its effect cancels out when computing EWs.

The resulting value of $\simeq 1.4$ for A_V is in good agreement with the value of 1.6 obtained by Ressler et al. (2010). Our estimations are also consistent with the colour excess obtained from the nebular extinction coefficient derived from the CAFOS spectrum ($E(B–V)$= 0.66, see Sect. 2). We note that the colour excess derived from the best fit is slightly higher than the previous values proposed in the literature, which ranges from 0.44 to 0.5 (Seaton 1980; Feibelman 1997).

We also note that while the bump at 2200 Å is successfully reproduced, the fitting around ~1600 Å does not reach the intensity levels of the observed spectrum. This can be a consequence of the parameterization used, since only a value of R_V has been taken into account. Besides, the lack of an accurate knowledge about the behavior of the extinction laws in this spectral range makes it difficult this kind of analysis.

Table 3. Stellar parameters of the two components of BD+30°623.

Stellar parameters	Cool Star	Hot star
$T_{\rm eff}$ [K]	9850 ± 150	90000 ± 10000
$\log g$	3.5± 0.25	5.5± 0.1
$M/{\rm M}_\odot$	0.55 ± 0.02	0.56 ± 0.03
$R/{\rm R}_\odot$	2.1± 0.6	0.22± 0.03
$\log(L/{\rm L}_\odot)$	1.60 ± 0.25	3.4 ± 0.2
R_V	2.3 ± 0.1	
$E(B-V)$	0.60 ± 0.05	
d [pc]	285 ± 85	

5 DISCUSSION

The spectral analysis described above provides values of the $T_{\rm eff}$ and gravities of both components of BD+30°623. While it is true that the $T_{\rm eff(cool)}$ has been already determined in a quite accurately way by several authors (see above), this is the first time that the parameters of the hot component have been spectroscopically derived. In Table 3 we list the results derived from the spectral analysis described in the previous sections ($T_{\rm eff}$ and gravities of the two components, and extinction) as well as the stellar parameters derived below from the evolutionary tracks (mass, radius, luminosity of the two components and the distance to the system). Note that the $T_{\rm eff(hot)}$ is not an strict average of the $T_{\rm eff}$ listed in Table 2, we prefer to give a round number that represents all the solutions with an uncertainty bracketing all of them. Also note that the error in $\log g_{\rm hot}$ comes from an average of the different values of the $\log g$ of the models that have passed all the filters in the analysis. In what follows, we adopt between the seven successful solutions matching the observed spectrum, that shown in Fig. 5, namely, $T_{\rm eff(hot)}$ = 90000 K, $\log g_{\rm hot} = 5.6$, $T_{\rm teff(cool)} = 9850$ K and $\log g_{\rm cool} = 3.5$. These parameters allow us to compare with the appropriate evolutionary tracks and isochrones.

Fig. 7 shows the position of the hot component of BD+30°623 in the HR diagrams $\log g_* - T_{\rm eff}$ (top) and $\log(L_*/{\rm L}_\odot) - T_{\rm eff}$ (bottom) on the evolutionary tracks for post-AGB tracks by Blöcker (1995). The location of the star is consistent with a mass of $M_{\rm hot} = 0.56 \pm 0.03$ M$_\odot$, which implies a radius $R_{\rm hot} = 0.22 \pm 0.03$ R$_\odot$, and a luminosity $\log(L_{\rm hot}/{\rm L}_\odot) = 3.4 \pm 0.2$. The luminosity and the dereddened integrated flux of the model fitting this component lead to a distance $d_{\rm hot}$=253±88 pc. The derived stellar mass indicates a progenitor of ~ 1 M$_\odot$ in the main sequence and, therefore, an age of about 10^9– 10^{10} yr. The parameters derived from the evolutionary tracks agree with those typical of sdOs (Oreiro et al. 2004; Geiger et al. 2011). Also, the narrowness of the He II λ4686 absorption line is compatible with an sdO classification (as previously pro-

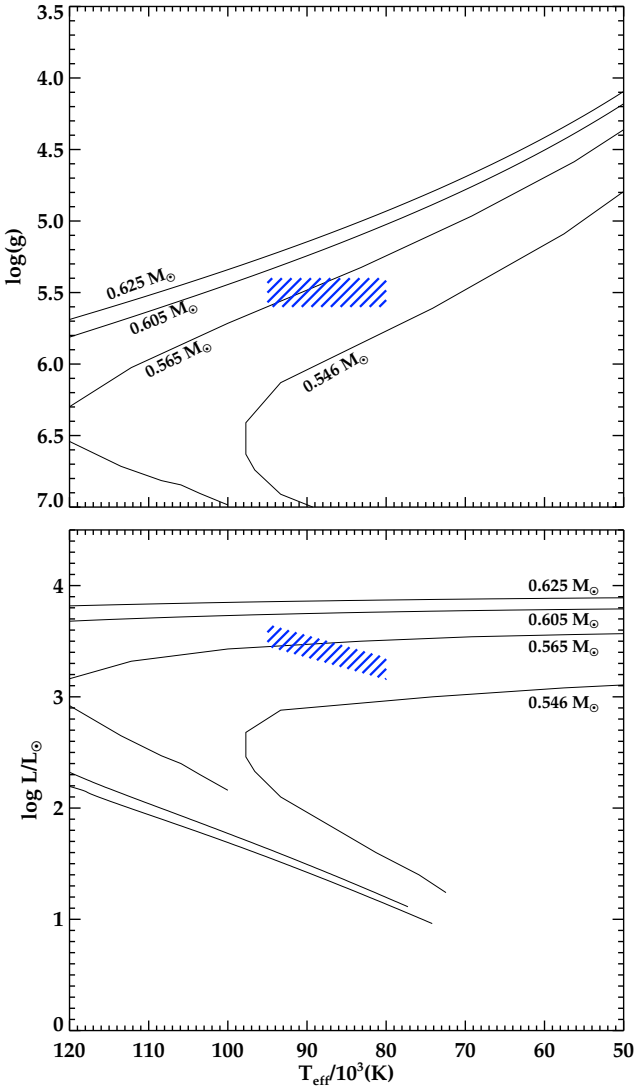

Figure 7. Location of the hot component on the evolutionary tracks by Blöcker (1995). The blue solid lines indicates the region of the possible parameters of the hot star derived from the final solutions. Each evolutionary track is labelled with the corresponding stellar mass (in $M_\odot$).

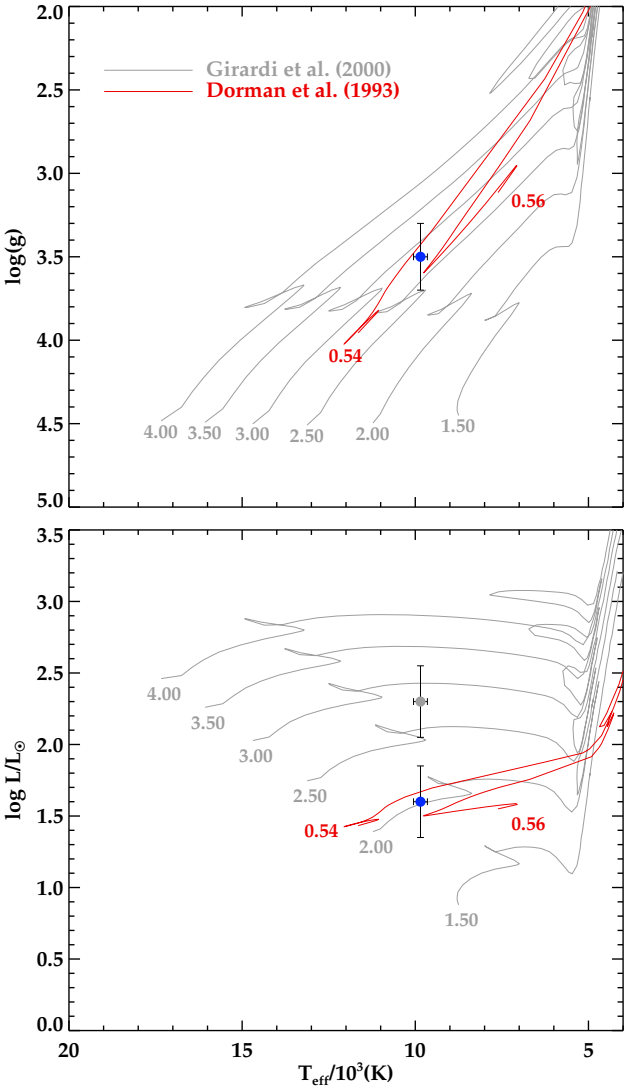

Figure 8. Location of the cool component on the evolutionary tracks calculated by Girardi et al. (2000) (grey lines) and the post-HB evolutionary tracks by Dorman et al. (1993) (red lines). Each evolutionary track is labelled with the corresponding stellar mass (in $M_\odot$). The location of the cool component in the top panel corresponds to two positions in the bottom panel depending on the evolutionary track with which we are comparing it (see the text).

posed by e.g. Kohoutek 1967, Greenstein 1972), rather than with a white dwarf. However, other classifications (like, e.g, O(He)-type) may also be compatible. Therefore, an analysis of high-resolution spectra in the UV range, as that carried out by Latour et al. (2013) for the sdO BD+28 4211, could allow us to confirm or rule out a possible sdO classification.

Fig. 8 shows the position of the cool component in the HR diagrams $\log g_* - T_{\rm eff}$ (top) and $\log(L_*/L_\odot) - T_{\rm eff}$ (bottom) on the post main-sequence evolutionary tracks by Girardi et al. (2000) with $Z = 0.004$ (grey) and the post-HB evolutionary tracks by Dorman et al. (1993) with $Z = 0.006$ (red). The stellar parameters derived are compatible, a priori, with two possible scenarios: an A0 star ascending the giant branch and a A0 star in the HB.

In the hypothesis that the cool component were an A0 star ascending the giant brach, the comparison with the Girardi et al. (2000) tracks gives a mass $M_{\rm cool} = 2.9 \pm 0.5$ $M_\odot$, which implies a radius $R_{\rm cool} = 4.9 \pm 1.5$ $R_\odot$, a luminosity $\log(L_{\rm cool}/L_\odot) = 2.3 \pm 0.3$ and an age ~ 300 Myr. These parameters lead to a number of inconsistencies when compared with those of the hot star. If the CS is a physical pair, the age of the cool star is incompatible with the much longer time span required by the hot star to reach its current evolutionary status. Therefore, interaction between the stars (e.g., mass transfer) should be invoked to explain the age difference. This inconsistency in the age has been already reported for other similar CSs (see e.g., NGC 3132, Ciardullo et al. 1999). However, the luminosity and the dereddened integrated flux of the cool star lead to a distance $d_{\rm cool}$=710±280 pc that is incompatible with the CS being a physical binary but a coincidental alignment. This scenario is also difficult to reconcile with the observations. In particular, it would be hard to explain that the Hubble Space Telescope does not resolve the pair, *and, simultaneously,* that the mean radial velocity of the cool star ($V_{\rm LSR}$ = +47.6±1.6 km s^{-1}) and the systemic velocity of the nebula ($V_{\rm LSR}$ = +41±5 km s^{-1}) are in agreement (Greenstein

1972). In addition, the complex nebular morphology is difficult to understand within a single-star hypothesis but strongly suggests the presence of a binary system (see below). Moreover, the radii derived from the evolutionary tracks yield a value of 0.002 for the parameter a, defined as $(R_{\rm hot}/R_{\rm cool})^2$ under the assumption that both components form a binary system (eq. 1); that value is a factor of 6.0 lower than the mean value a=0.012 obtained from the spectral analysis (Table 2). In view of all these arguments we can discard the scenario of the cool component being a giant-branch star.

Alternatively, in the hypothesis that the cool component were an A0 star in the HB, the comparison with the Dorman et al. (1993) tracks gives a mass $M_{\rm cool}$ = 0.55 ± 0.02 $M_\odot$ (Fig. 8, red lines), $R_{\rm cool}$ = 2.1 ± 0.6 $R_\odot$ and $\log(L_{\rm cool}/L_\odot) = 1.60 \pm 0.25$. The luminosity and the dereddened integrated flux lead to a distance $d_{\rm cool}$=294±69 pc that agrees very well with that derived above for the hot component ($d_{\rm hot}$=253±88 pc) and is compatible with both stars forming a binary system. Moreover, in contrast with the giant-branch scenario, the radius derived for the HB star gives a = 0.011, in very good agreement with the mean value of a obtained from the spectral analysis (see Sect. 4). Besides, the normalization constant between the best fitting models and the observed spectrum is $k_{\rm norm} \simeq 2.77 \times 10^{-20}$, which is defined as $(R_{\rm cool}/d)^2$ (eq. 1). Taking $R_{\rm cool} = 2.1$ we obtain a distance to the system d=285±85 pc, in agreement with the values derived independently for each component. This result also agrees with the range 200-300 pc considered by Ressler et al. (2010) based on the Hipparcos parallax (185 pc) and, alternatively, on the observed m_V magnitude and the assumption that the cool star is an HB A star with $M_V \simeq 1.0$ (240 pc). The fact that we obtain a very similar distance from an independent way –in our case, a spectral analysis– strongly reinforces the validity of our results. Finally, it should be noted that the parallax from the Hipparcos catalogue is $\pi = 5.40 \pm 1.70$ mas and the new reduction of the Hipparcos astrometric data by van Leeuwen (2007) provides $\pi = 3.79 \pm 1.61$ mas. In both cases $\sigma_\pi/\pi > 0.17$ and the Lutz-Kelker bias (Lutz & Kelker 1973) prevents from using the Hipparcos parallax to obtain a reliable distance.

Concerning the age of the cool component, we note that the Dorman et al. (1993) evolutionary tracks do not provide neither the masses of the progenitor stars in the main sequence (ZAMS) nor their current ages. However, according to the evolutionary models by Serenelly & Weiss (2005), stars with masses between 0.8 and 0.9 $M_\odot$ in the ZAMS might evolve (depending on the metallicity and the mass loss) to HB stars with masses around 0.55 $M_\odot$ –as it is our case– in periods between 8 and 12 Gyr. This range of ages is comparable to the age estimated for the hot component of BD+30°623. Therefore, the classification of the cool component as an HB A0 star is completely coherent with both the spectral analysis and the subsequent evolutionary study based on tracks and isochrones.

Another interesting point is the complex morphology of NGC 1514, consisting of numerous bubbles in the optical range (see Fig. 1) and a pair of axisymmetric rings recently discovered at mid-infrared wavelengths (Ressler et al. 2010). As mentioned above, a binary nature of BD+30°623 could already be tentatively inferred from this complex morphology, since binary interactions are generally believed to be the origin of non-spherical structures in PNe (see, e.g., Miszalski et al. 2009; de Marco 2009). It is true that neither radial velocity variations nor photometric and spectroscopic variability have been found in BD+30°623 (Greenstein 1972; Purgathofer & Schnell 1983, see also Sect. 2.2), which does not favor an association. However, in our case, the binary could be relatively close or have evolved through a common envelope phase (see Muthu & Anandarao 2003) but being observed pole-on (or nearly) so that no variability can be observed whereas binary interactions can shape the complex nebula. We note that a pole-on binary is compatible with the narrowness of the absorption lines in the A0 star reported by Greenstein (1972), who concluded that the rotational velocity has to be small ($\leqslant 40\,{\rm km\,s^{-1}}$). Alternatively, the pair could be a wide binary. This scenario would explain the lack of variability but have difficulties to account for the nebular complexity, unless particular orbital properties are considered (e.g., a highly eccentric orbit). In any case, conclusions about the characteristics of the binary and its relationship to nebular shaping should await for higher-resolution images of this object.

NGC 1514 is not unique among PNe and cases of PNe with "cool" CSs are well known (Lutz 1979, de Marco 2009). In particular, He 2-36, NGC 2346, NGC 3132, and PC 11 (Méndez 1978; Pereira et al. 2010) contain an A-type star like NGC 1514. Moreover, most of these PNe present bipolar or complex morphologies that are much easier to explain in a binary scenario than in a single star one. We note that the knowledge of the stellar parameters for the hot components in these peculiar CSPNe is very scarce and the analysis of these CSs has been mainly focused on the cool components (see Table 4 in de Marco 2009). In this context, the detailed spectral analysis presented in this work introduces a remarkable improvement since it allows us to obtain the stellar parameters of both cool and hot component simultaneously. Besides, this kind of analysis is useful to refine the spectral classification and the evolutionary status of the cool components in these systems. The future application of this method to similar peculiar CSs will be highly interesting to search for common properties in these systems and to constrain the formation and evolution of these enigmatic pairs of stars.

6 CONCLUSIONS

We have analysed ultraviolet IUE and CAFOS optical spectra of BD+30°623, the peculiar binary central star of NGC 1514. BD+30°623 shows an unusual central star spectrum whose main features correspond to an A-type star but also presents He II lines that must originate in a much hotter companion. Previous studies of this central star have been unable to provide unambiguous parameters for its two components. Making use of state-of-the-art model-atmospheres for hot, compact stars (Tübingen NLTE - Model Atmosphere Package) and Kurucz synthetic models, we have carried out a detailed analysis of the ultraviolet and optical spectra with the aim of constraining the properties of this object. Grids of composite models of a cool+hot star were built. A χ^2-fit and an iterative procedure based on filters imposed by observational constraints was devised to find the solutions that best reproduce both the shape of the ultraviolet and optical continuum and the main spectral features. To our knowledge, this kind of detailed analysis has not been done before for any of the peculiar binary central stars. The main results of this work can be summarized as follows:

1. The spectroscopic analysis leads to $T_{\rm eff(cool)} = 9850 \pm 150$ K, $\log g_{\rm cool} = 3.50 \pm 0.25$ and [M/H]$\simeq -0.5$. For the hot component, solutions for $T_{\rm eff(hot)}$ between 80000 K and 95000 K, $\log g_{\rm hot}$ between 5.4 and 5.6 and compositions pointing to a helium-rich star were found. An unique value for the extinction towards the two stars has been assumed, namely, $R_V = 2.3 \pm 0.1$ and $E(B–V) = 0.60 \pm 0.05$. Besides, the extinction coefficient derived from the nebular spectrum is $c(\mathrm{H}\beta) \simeq 0.97$.

2. By comparing the stellar parameters derived for both components with the appropriate evolutionary tracks, we conclude that

the cool component is compatible with an Horizontal-Branch A0 star with mass $M_{\rm cool} = 0.55 \pm 0.02$ M$_\odot$, radius $R_{\rm cool} = 2.1 \pm 0.6$ R$_\odot$ and luminosity $\log(L_{\rm cool}/{\rm L}_\odot) = 1.60 \pm 0.25$. A distance $d_{\rm cool}$=294±69 pc is also derived. In the hypothesis underlying all this work that the stars form a physical pair, the scenario with an A0 star ascending the giant branch proposed by other authors seems to be inconsistent and therefore, should be discarded. On the other hand, the parameters of the hot component are $M_{\rm hot} = 0.56 \pm 0.03$ M$_\odot$, $R_{\rm hot} = 0.22 \pm 0.03$ R$_\odot$, and $\log(L_{\rm cool}/{\rm L}_\odot) = 3.4 \pm 0.2$. A distance of $d_{\rm hot}$=253±88 pc is derived. Although an sdO nature seems to be the most plausible one for this component, it is difficult to establish this classification firmly without high-resolution observations. The analysis is compatible with the two stars forming a physical pair.

3. A reanalysis of the IUE spectra shows that no variability is seen at short wavelengths, in contrast with the variation of the continuum flux by a factor of ∼2 reported by Feibelman (1997).

The analysis presented in this paper improves noticeably previous studies carried out for this object. However, further observations, like high-resolution spectra, will help to determine with a better accuracy parameters such as the metal abundance of the cool component and the rotation velocities. New long- and short-term observations would be also required in order to study the possible variability of this system and the properties of the binary. Theoretical studies addressing the evolution of this kind of systems are also imperative.

ACKNOWLEDGMENTS

We are very grateful to our anonymous referee for his/her comments that have improved the discussion of the paper. This work has been partially supported by grant AYA 2011-24052 (AA, ES), AYA2011-26202 (BM), and AYA 2011-30228-C3-01 (LFM) of the Spanish MINECO, and by grant INCITE09 312191PR (AA, LFM, AU) of Xunta de Galicia, all of them partially funded by FEDER funds, and by grant 12VI20 (AA, LFM, AU) of the University of Vigo. The authors thank Nicole Reindl for her helpful suggestions regarding the TMAP models, and Jesús Maíz-Apellaniz for discussions about the extinction. The TMAW service (http://astro-uni-tuebingen.de/∼TMAW) used to calculate theoretical spectra for this paper was constructed as part of the activities of the German Astrophysical Virtual Observatory. Authors also acknowledge the Calar Alto Observatory for the service observations. We acknowledge support from the Faculty of the European Space Astronomy Centre (ESAC). This research is based on INES data from the IUE satellite. The INES archive is supported by the Spanish Virtual Observatory through grant AYA2011-24052. We have also made use of the SIMBAD database, operated at the CDS, Strasbourg (France), Aladin and NASAs Astrophysics Data System Bibliographic Services.

REFERENCES

Bertone E., Buzzoni A., Chávez M., Rodríguez-Merino L. H., 2004, AJ, 128, 829
Blöcker T., 1995, A&A, 299, 755
Castelli F. & Kurucz R. L., 2003, in N. Piskunov, W. W. Weiss and D.F. grey, eds., Proc. IAU Symp. 210, Modelling of Stellar Atmospheres, Astronomical Society of the Pacific, poster A20
Chopinet M., 1963, JO, 46, 27
Ciardullo R., Bond H. E., Sipior M. S., Fullton L. K., Zhang C.-Y., Schaefer K. G., 1999, AJ, 118, 488
De Marco O., 2009, PASP, 121, 316
De Marco O., Passy J. C., Frew D. J., Moe M., Jacoby G. H., 2013, MNRAS, 428, 2118
Dorman B., Rood R. T., O'Connell R. W., 1993, ApJ, 419, 596
Eisenstein D. J., et al., 2006, AJ, 132, 676
Feibelman W. A., 1997, PASP, 109, 659
Fitzpatrick E. L., 1999, PASP, 111, 63
Frew D. J., Parker Q. A., 2010, PASA, 27, 129
Geier S., et al., 2011, AIPC, 1331, 163
Girardi L., Bressan A., Bertelli G., Chiosi C., 2000, A&AS, 141, 371
Gray R. O. & Corbally C. J. 2009, Stellar Spectral Classification, Princeton University Press
Greenstein J. L., 1972, ApJ, 173, 367
Grewing M., Neri R., 1990, A&A, 236, 223
Kaler J. B., 1976, ApJS, 31, 517
Kohoutek L., 1967, BAICz, 18, 103
Kohoutek L., Hekela J., 1967, BAICz, 18, 203
Kondo Y., Boggess A., Maran S. P., 1989, ARA&A, 27, 397
Kurucz R.L. 1993, ATLAS9 Stellar Atmosphere Programs and 2 km/s grid. CD-ROM No. 13. Cambridge, Massachusetts, Smithsonian Astrophysical Observatory
Latour M., Fontaine G., Chayer P., Brassard P., 2013, ApJ, 773, 84
Lutz J. H., 1977, A&A, 60, 93
Lutz T. E., Kelker D. H., 1973, PASP, 85, 573
Mclaughlin D. B., 1942, PASP, 54, 31
Méndez R. H., 1978, MNRAS, 185, 647
Miszalski B., Acker A., Parker Q. A., Moffat A. F. J., 2009, A&A, 505, 249
Muthu C., 2001, BASI, 29, 381
Muthu C., Anandarao B. G., 2003, AJ, 126, 2963
Oreiro Rey R., Rodríguez López C., Ulla A., Pérez Hernáandez F., Garrido R., Manteiga M., MacDonald J., 2004, LNEA, 1, 133
Osterbrock D. E., 1989, Astrophysics of Gaseous Nebulae and Active Galactic Nuclei. Univ. Science Books, Mill Valley, CA
Payne C. H., 1930, Harvard College Observatory Bulletin, 878, 1
Pereira C. B., Baella N. O., Daflon S., Miranda L. F., 2010, A&A, 509, A13
Pottasch S.R., 1984, in Planetary nebulae, Dordrecht, D. Reidel Publishing Co.
Purgathofer A., Schnell A., 1983, IBVS, 2362, 1
Rauch T., Werner K., Ziegler M., Kruk J. W., Oliveira C. M., 2007, Asymmetrical Planetary Nebulae IV, http://www.iac.es/proyect/apn4, article #18
Rauch T., Werner K., Bohlin R., Kruk J. W., 2013, A&A, 560, A106
Ressler M. E., Cohen M., Wachter S., Hoard D. W., Mainzer A. K., Wright E. L., 2010, AJ, 140, 1882
Seares F. H., Hubble E. P., 1920, ApJ, 52, 8
Seaton M. J., 1979, MNRAS, 187, 73
Seaton M. J., 1980, QJRAS, 21, 229
Serenelli A., Weiss A., 2005, A&A, 442, 1041
Taranova O. G., Shenavrin V. I., 2007, AstL, 33, 584
van Leeuwen F., 2007, A&A, 474, 653
Weidmann W. A., Gamen R., 2011, A&A, 526, A6
Werner K., Deetjen J. L., Dreizler S., Nagel T., Rauch T., Schuh S. L., 2003, ASPC, 288, 31
Ziegler M., Rauch T., Werner K., Köppen J., Kruk J. W., 2012, A&A, 548, A109